

# Observables of Lattice Gauge Theory in Minkowski Space

Tamás S. Biró<sup>a</sup>, Harald Markum<sup>b</sup>, Rainer Pullirsch<sup>b,c</sup>, and Wolfgang Sakuler<sup>b</sup>

<sup>a</sup>Research Institute for Particle and Nuclear Physics, Hungarian Academy of Sciences, H-1525 Budapest, Hungary

<sup>b</sup>Atominstytut, Technische Universität Wien, A-1040 Vienna, Austria

<sup>c</sup>Institut für Theoretische Physik, Universität Regensburg, D-93040 Regensburg, Germany

U(1) gauge fields are decomposed into a monopole and photon part across the phase transition from the confinement to the Coulomb phase. We analyze the leading Lyapunov exponents of such gauge field configurations on the lattice which are initialized by quantum Monte Carlo simulations. We observe that the monopole field carries the same Lyapunov exponent as the original U(1) field. Evidence is found that monopole fields stay chaotic in the continuum whereas the photon fields are regular. First results are presented for the full spectrum of Lyapunov exponents of the U(1) gauge system.

## 1. Monopole and photon part of U(1) theory

We are interested in the relationship between monopoles and classical chaos across the phase transition at  $\beta_c \approx 1.01$ . We begin with a  $4d$  U(1) gauge theory described by the Euclidean action  $S\{U_l\} = \beta \sum_p (1 - \cos \theta_p)$ , where  $U_l = U_{x,\mu} = \exp(i\theta_{x,\mu})$  and  $\theta_p = \theta_{x,\mu} + \theta_{x+\hat{\mu},\nu} - \theta_{x+\hat{\nu},\mu} - \theta_{x,\nu}$ . Following Ref. [1], we have factorized our gauge configurations into monopole and photon fields. The U(1) plaquette angles  $\theta_{x,\mu\nu}$  are decomposed into the “physical” electromagnetic flux through the plaquette  $\bar{\theta}_{x,\mu\nu}$  and a number  $m_{x,\mu\nu}$  of Dirac strings through the plaquette

$$\theta_{x,\mu\nu} = \bar{\theta}_{x,\mu\nu} + 2\pi m_{x,\mu\nu}, \quad (1)$$

where  $\bar{\theta}_{x,\mu\nu} \in (-\pi, +\pi]$  and  $m_{x,\mu\nu} \neq 0$  is called a Dirac plaquette.

## 2. Classical chaotic dynamics from quantum Monte Carlo initial states

Chaotic dynamics in general is characterized by the spectrum of Lyapunov exponents. These exponents, if they are positive, reflect an exponential divergence of initially adjacent configurations. In case of symmetries inherent in the Hamiltonian of the system there are correspond-

ing zero values of these exponents. Finally negative exponents belong to irrelevant directions in the phase space: perturbation components in these directions die out exponentially. Pure gauge fields on the lattice show a characteristic Lyapunov spectrum consisting of one third of each kind of exponents [2]. Assuming this general structure of the Lyapunov spectrum we first investigate its magnitude, namely the maximal value of the Lyapunov exponent,  $L_{\max}$ .

The general definition of the Lyapunov exponent is based on a distance measure  $d(t)$  in phase space,

$$L := \lim_{t \rightarrow \infty} \lim_{d(0) \rightarrow 0} \frac{1}{t} \ln \frac{d(t)}{d(0)}. \quad (2)$$

In case of conservative dynamics the sum of all Lyapunov exponents is zero according to Liouville’s theorem,  $\sum L_i = 0$ . We utilize the gauge invariant distance measure consisting of the local differences of energy densities between two  $3d$  field configurations on the lattice:

$$d := \frac{1}{N_P} \sum_P |\text{tr} U_P - \text{tr} U'_P|. \quad (3)$$

Here the symbol  $\sum_P$  stands for the sum over all  $N_P$  plaquettes, so this distance is bound in the interval  $(0, 2N)$  for the group SU(N).  $U_P$  and  $U'_P$

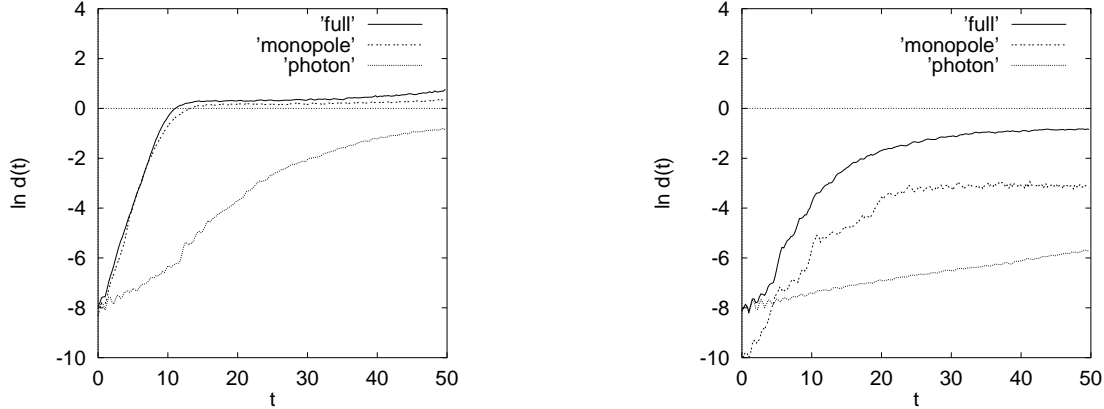


Figure 1. Exponentially diverging distance in real time of initially adjacent U(1) field configurations on a  $12^3$  lattice prepared at  $\beta = 0.9$  in the confinement (left) and at  $\beta = 1.1$  in the Coulomb phase (right).

are the familiar plaquette variables, constructed from the basic link variables  $U_{x,i}$ ,

$$U_{x,i} = \exp(aA_{x,i}T), \quad (4)$$

located on lattice links pointing from the position  $x = (x_1, x_2, x_3)$  to  $x + ae_i$ . The generator of the group  $U(1)$  is  $T = -ig$  and  $A_{x,i}$  is the vector potential. The elementary plaquette variable is constructed for a plaquette with a corner at  $x$  and lying in the  $ij$ -plane as  $U_{x,ij} = U_{x,i}U_{x+i,j}U_{x+j,i}^\dagger U_{x,j}^\dagger$ . It is related to the magnetic field strength  $B_{x,k}$ :

$$U_{x,ij} = \exp(\varepsilon_{ijk}a^2B_{x,k}T). \quad (5)$$

The electric field strength  $E_{x,i}$  is related to the canonically conjugate momentum  $P_{x,i} = a\dot{U}_{x,i}$  via

$$E_{x,i} = \frac{1}{g^2a^2} \left( T\dot{U}_{x,i}U_{x,i}^\dagger \right). \quad (6)$$

The Hamiltonian of the lattice gauge field system can be casted into the form

$$H = \sum \left[ \frac{1}{2} \langle P, P \rangle + 1 - \frac{1}{4} \langle U, V \rangle \right]. \quad (7)$$

Here the scalar product stands for  $\langle A, B \rangle = \text{Re}(AB^\dagger)$ . The staple variable  $V$  is a sum of triple products of elementary link variables closing a plaquette with the chosen link  $U$ . This way the Hamiltonian is formally written as a sum over link contributions and  $V$  plays the role of the classical force acting on the link variable  $U$ .

We prepare the initial field configurations from a standard four dimensional Euclidean Monte Carlo program on a  $12^3 \times 4$  lattice varying the inverse gauge coupling  $\beta$  [3]. We relate such four dimensional Euclidean lattice field configurations to Minkowskian momenta and fields for the three dimensional Hamiltonian simulation by selecting a fixed time slice of the four dimensional lattice.

### 3. Chaos, confinement and continuum limit

We start the presentation of our results with a characteristic example of the time evolution of the distance between initially adjacent configurations. An initial state prepared by a standard four dimensional Monte Carlo simulation is evolved according to the classical Hamiltonian dynamics in real time. Afterwards this initial state is rotated locally by group elements which are chosen randomly near to the unity. The time evolution of this slightly rotated configuration is then pursued and finally the distance between these two evolutions is calculated at the corresponding times. A typical exponential rise of this distance followed by a saturation can be inspected in Fig. 1 from an example of U(1) gauge theory in the confinement phase and in the Coulomb phase. While the saturation is an artifact of the compact distance measure of the lattice, the exponential rise (the linear rise of the logarithm) can be used for the determination of the leading Lyapunov expo-

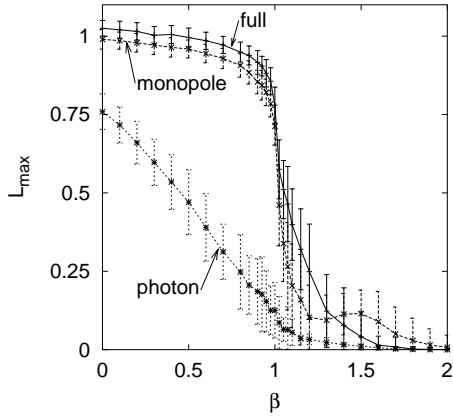


Figure 2. Lyapunov exponent of the decomposed U(1) fields as a function of coupling.

ment. The left plot exhibits that in the confinement phase the original field and its monopole part have similar Lyapunov exponents whereas the photon part has a smaller  $L_{max}$ . The right plot in the Coulomb phase suggests that all slopes and consequently the Lyapunov exponents of all fields decrease substantially.

The main result of the present study is the dependence of the leading Lyapunov exponent  $L_{max}$  on the inverse coupling strength  $\beta$ , displayed in Fig. 2. As expected the strong coupling phase is more chaotic. The transition reflects the critical coupling to the Coulomb phase. The plot shows that the monopole fields carry Lyapunov exponents of nearly the same size as the full U(1) fields. The photon fields yield a non-vanishing value in the confinement ascending toward  $\beta = 0$  for randomized fields which indicates that the decomposition works well only around the phase transition.

An interesting result concerning the continuum limit can be viewed from Fig. 3 which shows the energy dependence of the Lyapunov exponents for the U(1) theory and its components. One observes an approximately linear relation for the monopole part while a quadratic relation is suggested for the photon part in the weak coupling regime. From scaling arguments one expects a functional relationship between the Lyapunov ex-

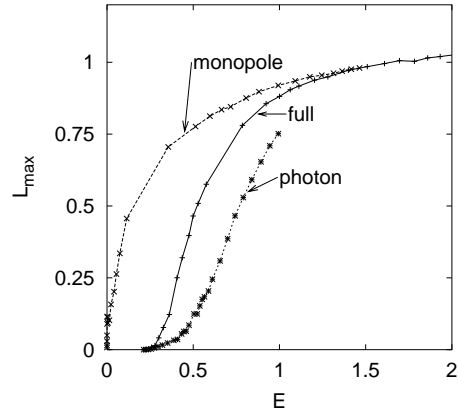


Figure 3. Comparison of average maximal Lyapunov exponents as a function of the scaled average energy per plaquette. The full U(1) theory shows an approximately quadratic behavior in the weak coupling regime which is more pronounced for the photon field. The monopole field indicates a linear relation.

ponent and the energy [2,4]

$$L(a) \propto a^{k-1} E^k(a), \quad (8)$$

with the exponent  $k$  being crucial for the continuum limit of the classical field theory. A value of  $k < 1$  leads to a divergent Lyapunov exponent, while  $k > 1$  yields a vanishing  $L$  in the continuum. The case  $k = 1$  is special allowing for a finite non-zero Lyapunov exponent. Our analysis of the scaling relation (8) gives evidence, that the classical compact U(1) lattice gauge theory and especially the photon field have  $k \approx 2$  and with  $L(a) \rightarrow 0$  a regular continuum theory. The monopole field signals  $k \approx 1$  and stays chaotic approaching the continuum.

#### 4. Spectrum of the stability matrix

Instead of the classical determination of the Lyapunov exponent, which has been calculated by the rescaling method in the preceding sections, we now use the monodromy matrix approach [5]. The Lyapunov spectrum  $L_i$  is expressed in terms of the eigenvalues  $\Lambda_i$  of the monodromy matrix

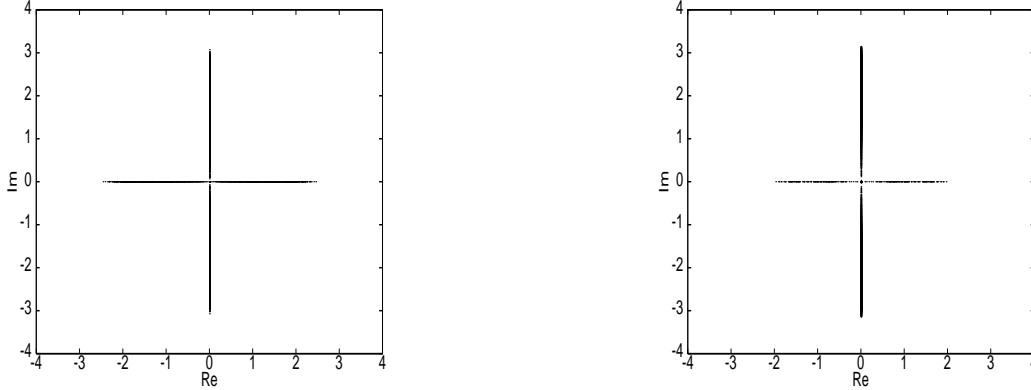


Figure 4. Full complex eigenvalue spectrum of the monodromy matrix for  $t = 0$  at  $\beta = 0.9$  in the confinement (left) and at  $\beta = 1.1$  in the Coulomb phase (right).

$M$ :

$$L_i = \lim_{t \rightarrow \infty} \frac{1}{t} \int_0^t \Lambda_i(t') dt', \quad i = 1, \dots, f, \quad (9)$$

where  $\Lambda_i(t)$  are the solutions of the characteristic equation for  $f$  degrees of freedom

$$\det(\Lambda_i(t)\mathbb{1} - M(t)) = 0 \quad (10)$$

at a given time  $t$ . Here  $M$  is the linear stability matrix,

$$M = \begin{pmatrix} \frac{\partial \dot{U}}{\partial U} & \frac{\partial \dot{U}}{\partial P} \\ \frac{\partial \dot{P}}{\partial U} & \frac{\partial \dot{P}}{\partial P} \end{pmatrix} = \begin{pmatrix} 0 & 1 \\ -\frac{\partial^2 S_3}{\partial U^2} & 0 \end{pmatrix}, \quad (11)$$

with the three dimensional lattice action  $S_3$ .

Figure 4 displays the complex eigenvalues for selected configurations prepared by a quantum Monte Carlo heat-bath algorithm. In the confinement phase ( $\beta = 0.9$ ) the eigenvalues lie on either the real or on the imaginary axes. This is a nice illustration of a strange attractor of a chaotic system. Positive Lyapunov exponents eject the trajectories from oscillating orbits provided by the imaginary eigenvalues. Negative Lyapunov exponents attract the trajectories keeping them confined in the basin. In the Coulomb phase ( $\beta = 1.1$ ) the real Lyapunov exponents become rare to eventually vanish in the continuum limit

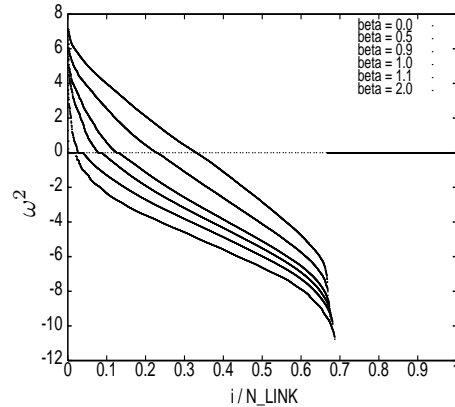


Figure 5. Real part of the squared spectrum of the stability matrix decreasing with increasing  $\beta$ .

(see Fig. 3). In all cases the spectrum is symmetric with respect to the real and imaginary axes: the former property is due to the fact that the equations of motion are real, the latter is due to the Hamiltonian being conservative (time independent). Also a number of zero-frequency modes occur which is connected to symmetry transformations commuting (in the Poisson bracket sense) with the Hamiltonian, such as time independent gauge transformations.

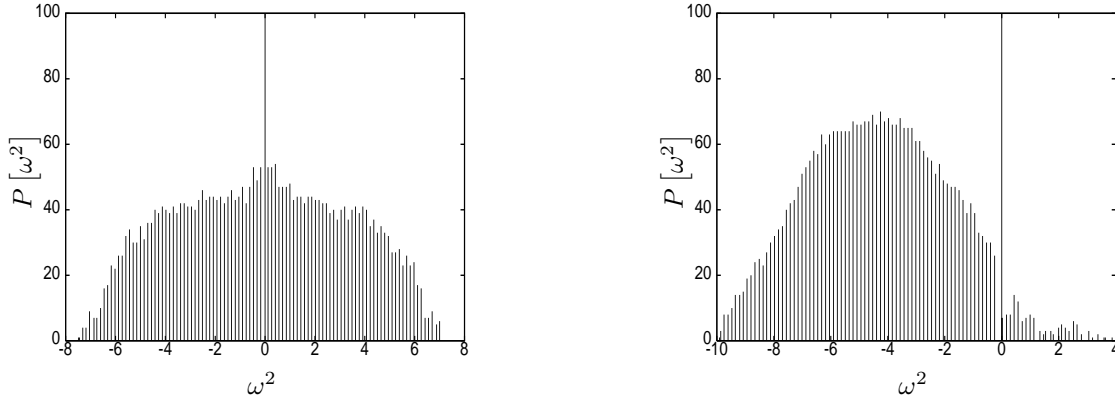


Figure 6. Power spectrum at  $\beta = 0$  (left) and at  $\beta = 1.1$  in the Coulomb phase (right).

Figure 5 shows the real part of the squared Lyapunov spectrum for several couplings. The overall pattern is similar to that obtained earlier for SU(2) studies with random configurations [5]. It exhibits an increasing number of zero modes with increasing  $\beta$ . Figure 6 gives insight into the distribution of the squared eigenvalues which is symmetric for  $\beta = 0$  and is shifted to negative values towards the Coulomb phase.

## 5. Summary

This contribution was devoted to the relation between monopoles, Lyapunov exponents and confinement in a (classical) compact U(1) theory. A decomposition into a monopole and photon part showed that the monopole field carries the same Lyapunov exponent as the original U(1) field. In the continuum limit the photon and U(1) fields behave regularly while the monopole part stays chaotic. This was substantiated by the spectrum of the monodromy matrix exhibiting an interplay between positive, imaginary and negative Lyapunov exponents in the confinement phase changing to a pure imaginary spectrum deep in the Coulomb phase leading to the regularity of the Maxwell theory. It will be interesting to compute the spectrum of the stability matrix on the photon and monopole part of the U(1) field. An

analysis of the behavior of the monopoles in the classical U(1) theory in Minkowski space is a challenge by itself.

## REFERENCES

1. J.D. Stack and R.J. Wensley, Nucl. Phys. B371 (1992) 597; T. Suzuki, S. Kitahara, T. Okude, F. Shoji, K. Moroda, and O. Miyamura, Nucl. Phys. B (Proc. Suppl.) 47 (1996) 374.
2. T.S. Biró, S.G. Matinyan, and B. Müller: Chaos and Gauge Field Theory, World Scientific, Singapore, 1995.
3. T.S. Biró, M. Feurstein, and H. Markum, APH Heavy Ion Physics 7 (1998) 235; T.S. Biró, N. Hörmann, H. Markum, and R. Pullirsch, Nucl. Phys. B (Proc. Suppl.) 86 (2000) 403; H. Markum, R. Pullirsch, and W. Sakuler, hep-lat/0201001; hep-lat/0205003; hep-lat/0209039.
4. L. Casetti, R. Gatto, and M. Pettini, J. Phys. A32 (1999) 3055; H.B. Nielsen, H.H. Rugh, and S.E. Rugh, ICHEP96 1603, hep-th/9611128; B. Müller, chaos-dyn/9607001; H.B. Nielsen, H.H. Rugh, and S.E. Rugh, chaos-dyn/9605013.
5. Á. Fülöp and T.S. Biró, Phys. Rev. C64 (2001) 064902.